13th World Conference on Earthquake Engineering
Vancouver, B.C., Canada
August 1-6, 2004
Paper No. 410

THREE-DIMENSIONAL TOPOGRAPHIC EFFECTS ON THE SEISMIC RESPONSE OF A EXTRADOSED BRIDGE

Jang Seok YI[1], Eu Kyeong CHO[2], Mo Seh KIM[3], Jae Kwan KIM[4]

SUMMARY

The seismic responses of a three-span extradosed bridge that is constructed at the site of irregular topography are investigated. The sub-surface topography is assumed to be irregular in longitudinal direction but regular in transverse direction. The ground of 3-D irregular geometry is modeled using 3-dimensional hyperelement formulated in Cartesian coordinate system. Amplification of ground motion occurs by the site effects and this is pronounced at the location of soft soil along the fault. The bridge structure is modeled using 3-D frame elements and the cables by elastic catenary elements. Three-dimensional seismic responses of bridge model subjected to ground motion acting in both longitudinal and transverse directions are obtained. It is found that spatial variation and soil-structure interaction have significant influence on the seismic responses of bridge.

INTRODUCTION

The spatial variability of ground motion has been investigated in terms of phase difference of traveling waves. But the wave passage effect does not seem to be very significant compared with the effects of site conditions on the ground motion. Spatially varying local soil profiles have influence on the change of amplitude and frequency content of the bedrock motion as it propagate upward and this site effect is known to have the dominant influence on the responses of the bridge[1]. The soft surface soil layer tends to amplify the intensity of ground motion and the bedrock motions are expected to be modified by the soft soil deposit resulting in lower frequency motions at ground surface which are believed to be critical for long period structures such as long-span bridges[2]. Resonance amplification can occur when the soil frequency is close to one of the important natural frequencies of bridge and the strongest local site amplification effects can be observed for the forces and displacements of the piers where the soft soil is located[3]. Moreover the structural response may be altered due to the soil-structure interaction. Hence many researchers have attempted to investigate these effects on the seismic response of long span bridges but their efforts have been limited to study using two-dimensional models because of computational difficulty involved in 3-D modeling. Several researchers found that soil-structure interaction can

[1] Senior Engineer, Hyundai Engineering & Construction Co., Seoul, Korea. Email:yijs@netian.com
[2] Chief Engineer, Hyundai Engineering & Construction Co., Seoul, Korea.
[3] Engineer, Hyundai Engineering & Construction Co., Seoul, Korea.
[4] Associate Professor, Seoul National University, Seoul, Korea.

contribute to the response to some degree. However it appears that more systematic study is in demand. The difficulty of the comprehensive study is due to the lack of analysis method that can model the ground of bridge site in 3-dimensional space. 3-dimensional hyper-element method formulated in 3-D Cartesian coordinate system has been proposed[4]. It can model the ground that has irregular surface topography and heterogeneous soil layers in longitudinal direction. Many bridge sites may belong to such a category. By combining the hyper-element model of ground with finite element model of bridge structure, the seismic response of bridges located in the irregular site can be obtained that account for the site effects and soil-structure interaction not only in longitudinal direction but also in transverse direction.

The developed tool is applied to the study of the seismic response of a three-span extradosed bridge that is constructed at the site that has heterogeneous soil profile in longitudinal direction but regular in transverse direction. The bridge structure is modeled using 3-D frame elements. The elastic catenary elements are employed for the cables. 3-D seismic responses of the bridge model subjected to ground motion acting in both longitudinal and transverse directions are obtained.

3-D HOMOGENEOUS HYPERELEMENT

Introduction

A three-dimensional transmitting boundary is formulated in Cartesian coordinate system. It is developed for the dynamic soil-structure interaction problems of arbitrary shape foundations in laterally heterogeneous strata overlying rigid bedrock as Figure 1. The ground is assumed a layered stratum over rigid bedrock. Instead of seeking an exact solution on the wave propagation in the layered strata, a semi-analytic approach is adopted that was first introduced by Waas[5] for the development of consistent transmitting boundaries for 2-dimensional regions and 3-dimensional axisymmetric regions.

The scattered wave field is assumed periodic in one axis direction and it is equivalent to the assumption that identical sources are arranged infinitely with the same period. But the repeating sources introduce distortion to the scattered wave field. There will be contamination coming from the adjacent sources. But if the period is sufficiently large then the solutions will converge to the true one. A novel coordinate transform is employed to uncouple the governing equation in Cartesian coordinate system.

The dynamic behavior of foundations of arbitrary shape can be analyzed by a hybrid approach in which the finite region including foundation is modeled by conventional finite element method and the surrounding infinite region by the developed transmitting boundary.

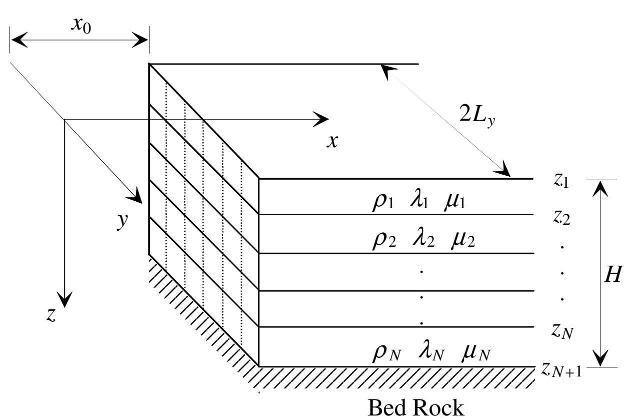

Fig. 1 Transmitting boundary located at $x = x_0$.

Formulation[4]

Let $\boldsymbol{\Gamma}$ be the vector of modal participation factors, then $\overline{\mathbf{P}}$ the vector of nodal line forces may be expressed as

$$\overline{\mathbf{P}} = [\mathbf{D\Phi} + \mathbf{L\Psi} - \mathbf{NX} + \mathbf{QZ}]\mathbf{E\Gamma} \tag{1}$$

where $\boldsymbol{\Phi}$, $\boldsymbol{\Psi}$, $\mathbf{X}$ and $\mathbf{Z}$ are the matrices of which the lth column vectors are $\boldsymbol{\Phi}^l$, $\boldsymbol{\Psi}^l$, $\mathbf{X}^l$ and $\mathbf{Z}^l$ respectively and $\mathbf{E}$ is the diagonal matrix of which the lth elements are defined by the expression,

$$E_{l,l} = e^{-ik_x x_0} = e^{-ik_{nx}^l x_0} \tag{2}$$

The symmetric or anti-symmetric nodal line displacement vector can be expressed as a linear combination of 3*N* modes:

$$\overline{\mathbf{U}} = \mathbf{YE\Gamma} \tag{3}$$

where $\overline{\mathbf{U}}$ is the vector of nodal line displacements and the lth column vector of the matrix $\mathbf{Y}$ is the displacement vector corresponding to the lth mode. By eliminating the vector of the participation factors from the equations (1) and (3), the dynamic stiffness matrix of the nth Fourier series term is obtained.

$$\overline{\mathbf{P}} = \overline{\mathbf{K}}\,\overline{\mathbf{U}} = [\mathbf{D\Phi} + \mathbf{L\Psi} - \mathbf{NX} + \mathbf{QZ}]\mathbf{Y}^{-1}\overline{\mathbf{U}} \tag{4}$$

The dynamic stiffness matrix $\overline{\mathbf{K}}$ is independent of the horizontal location x_0 and is a symmetric complex matrix. In fact, $\overline{\mathbf{K}}$ in (4) defines the displacement vector and force vector corresponding to the nth Fourier Series term. Therefore in order to be coupled with three-dimensional solid finite element model, $\overline{\mathbf{K}}$ in (4) need be transformed into a dynamic stiffness matrix defining the relation between nodal displacement vector and nodal force vector. Employing virtual work principle,

$$\mathbf{P}_e = \mathbf{K}_e^{+}\mathbf{U}_e = \left[\sum_{n=0}^{\infty}\left(\frac{1}{L_y}\right)\left(1-\frac{1}{2}\delta_{n0}\right)\mathbf{S}_n^T\mathbf{K}_n\mathbf{S}_n + \sum_{n=0}^{\infty}\left(\frac{1}{L_y}\right)\left(1-\frac{1}{2}\delta_{n0}\right)\mathbf{A}_n^T\mathbf{K}_n\mathbf{A}_n\right]\mathbf{U}_e \tag{5}$$

where $\mathbf{K}_n$ is the dynamic stiffness matrix from Eq. (4). The boundary which transmits energy into x<0 direction can be derived following the same procedure. However, the stiffness matrix $\mathbf{K}_e^{-}$ for the transmitting boundary for x<0 direction can be obtained conveniently from the relations between the modes propagating into x>0 and x<0 directions:

$$\mathbf{K}_e^{-} = \mathbf{I}\mathbf{K}_e^{+}\mathbf{I} \tag{6}$$

where matrix $\mathbf{K}_e^{+}$ is the same as given by (5) and $\mathbf{I}$ is a 3*N*×3*N* diagonal matrix of which elements are defined as $\mathbf{I}_{3j-2,3j-2} = -1$; $\mathbf{I}_{3j-1,3j-1} = 1$; and $\mathbf{I}_{3j,3j} = 1$.

3-D HOMOGENEOUS STRIP HYPERELEMENT

Introduction

The contiguous or adjacent foundations are always coupled through the soil. Hence their behavior is quite different due to the interaction effects between or among the foundations. The interaction effects can be very pronounced if the distance between them is very close. An 3-D homogeneous strip hyperelement[6] is developed to analyze the dynamic interaction between foundations. Since the hyperelement formulation utilizes wave modes in layered strata over rigid bedrock, it is very efficient computationally. Moreover, the present formulation in Cartesian coordinate system can model very efficiently the laterally inhomogeneous subgrade and the interaction between multiple foundations on it.

Formulation

The dynamic stiffness matrix of the rectangular region bounded by two vertical planes as Figure 2 can be derived as follows. Each layer of the stratum is assumed to consist of linearly elastic or viscoelastic isotropic homogeneous medium. The top surface of the stratum, the plane represented by $z = z_1$, is free of traction. The base of stratum at $z = z_{N+1} = H$ is assumed welded to the rigid bedrock. In $x_1 < x < x_2$ region, the propagation of wave in $+x$ and $-x$ direction both must be considered. The Fourier coefficient vector at $x = x_1$ and $x = x_2$ can be written as

$$\overline{\mathbf{U}}_1 = \mathbf{Y}\,\mathbf{E}(x_1)\mathbf{\Gamma}_1 + \mathbf{IY}\,\overline{\mathbf{E}}(x_1)\mathbf{\Gamma}_2 \tag{7.a}$$

$$\overline{\mathbf{U}}_2 = \mathbf{Y}\,\mathbf{E}(x_2)\mathbf{\Gamma}_1 + \mathbf{IY}\,\overline{\mathbf{E}}(x_2)\mathbf{\Gamma}_2 \tag{7.b}$$

where $\mathbf{\Gamma}_1$ and $\mathbf{\Gamma}_2$ are modal participation factors propagationg in $+x$ and $-x$ direction respectively. In $x = x_1$ and $x = x_2$, Fourier coefficient vector of nodal line force can be expressed as

$$\begin{aligned}\overline{\mathbf{P}}_1 =& [\mathbf{D\Phi} + \mathbf{L\Psi} - \mathbf{NX} + \mathbf{QZ}]\mathbf{E}(x_1)\mathbf{\Gamma}_1 \\ & - \mathbf{I}[\mathbf{D\Phi} + \mathbf{L\Psi} - \mathbf{NX} + \mathbf{QZ}]\overline{\mathbf{E}}(x_1)\mathbf{\Gamma}_2\end{aligned} \tag{8.a}$$

$$\begin{aligned}\overline{\mathbf{P}}_2 =& -[\mathbf{D\Phi} + \mathbf{L\Psi} - \mathbf{NX} + \mathbf{QZ}]\mathbf{E}(x_2)\mathbf{\Gamma}_1 \\ & + \mathbf{I}[\mathbf{D\Phi} + \mathbf{L\Psi} - \mathbf{NX} + \mathbf{QZ}]\overline{\mathbf{E}}(x_2)\mathbf{\Gamma}_2\end{aligned} \tag{8.b}$$

By eliminating $\mathbf{\Gamma}_1$, $\mathbf{\Gamma}_2$ from Eq. (7) and (8), the dynamic stiffness matrix about Fourier coefficient is obtained.

$$\begin{Bmatrix}\overline{\mathbf{P}}_1 \\ \overline{\mathbf{P}}_2\end{Bmatrix} = [\overline{\mathbf{K}}]\begin{Bmatrix}\overline{\mathbf{U}}_1 \\ \overline{\mathbf{U}}_2\end{Bmatrix} = \begin{bmatrix}\overline{\mathbf{K}}_{11} & \overline{\mathbf{K}}_{12} \\ \overline{\mathbf{K}}_{21} & \overline{\mathbf{K}}_{22}\end{bmatrix}\begin{Bmatrix}\overline{\mathbf{U}}_1 \\ \overline{\mathbf{U}}_2\end{Bmatrix} \tag{9}$$

Eq. (9) defines the displacement vector and force vector corresponding to the *n*th Fourier Series term. Therefore in order to be coupled with three-dimensional solid finite element model, $\overline{\mathbf{K}}$ need to be transformed into a dynamic stiffness matrix defining the relation between nodal displacement vector and nodal force vector. Employing virtual work principle,

$$\begin{Bmatrix}\mathbf{P}_{1e} \\ \mathbf{P}_{2e}\end{Bmatrix} = \left(\sum_{n=0}^{\infty}\mathbf{S}_n^T\mathbf{K}_n\left(\frac{2}{L_y}\right)\left(1-\frac{1}{2}\delta_{n0}\right)\mathbf{S}_n + \sum_{n=0}^{\infty}\mathbf{A}_n^T\mathbf{K}_n\left(\frac{2}{L_y}\right)\left(1-\frac{1}{2}\delta_{n0}\right)\mathbf{A}_n\right)\begin{Bmatrix}\mathbf{U}_{1e} \\ \mathbf{U}_{2e}\end{Bmatrix} \tag{10}$$

$$\begin{Bmatrix} \mathbf{P}_{1e} \\ \mathbf{P}_{2e} \end{Bmatrix} = \mathbf{K}_e \begin{Bmatrix} \mathbf{U}_{1e} \\ \mathbf{U}_{2e} \end{Bmatrix} \tag{11}$$

where $\mathbf{K}_n$ is the dynamic stiffness matrix from Eq. (9).

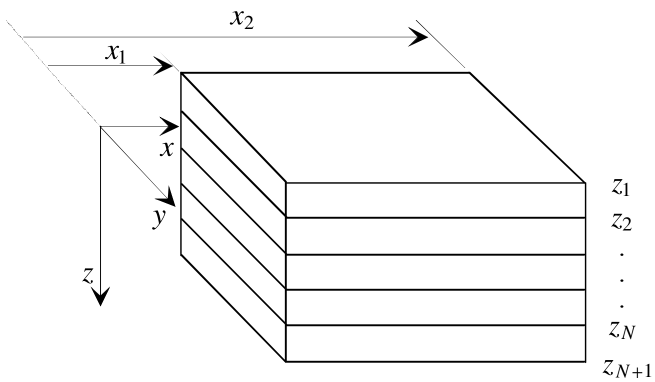

Fig. 2 $x_1 < x < x_2$ **rectangular region.**

EXTRADOSED BRIDGE AND MODELING

The extradosed system is a hybrid design that is a marriage between a concrete cable stressed girder bridge and a cable stayed bridge. In this new type of bridge, the wire carrying cables are placed outside the girders and up on the main concrete towers as opposed to inside the concrete boxes. However, the cables are not placed high up on tall towers, as would be the case with a conventional cable stayed bridge. With a typical cable stayed bridge most of the load (weight of the bridge deck, girders, cars and trucks) is carried through the cables, up to the top of the towers and then down through the towers to the foundations. In an extradosed bridge both the girders and the wire cables carry the load. A portion of the load is carried back through the girders to the towers and the remaining portion is carried by the cables up to the top of the towers and then back down through the towers to the foundations. As a result we have a very efficient load-carrying bridge with superior aesthetic qualities due to the exposed cables and concrete towers above the bridge roadway surface.

Figure 3 shows a three-span extradosed bridge supported by two main towers with a center span of 130 meters which constitutes part of a multi-span bridge crossing a strait. It is assumed that this part can be separated from the rest of the bridge.

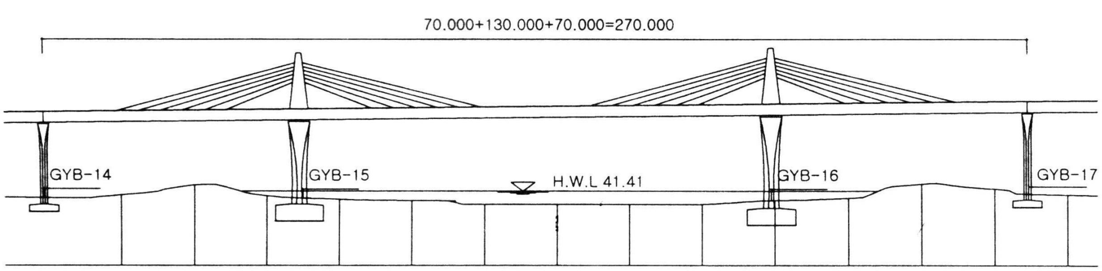

Fig. 3 Three span extradosed bridge.

This bridge is modeled using program HYUNSTAY[7]. In this program three-dimensional frame elements are used to model the deck and piers. Modeling girder, pier and pylon and bridge by this elements are shown in Figure 4. Geometric nonlinearity is considered in the process of formulation of the tangential stiffness matrix by Updated Lagrangian method[8]. Elastic catenary cable element that has 3-degrees of freedom per each node is used for modeling inclined cable. The cable is suspended between two fixed points and the Lagrangian coordinates of undeformed shape moves to the Lagrangian coordinates of deformed shape when the cable element undergoes deformation due to the self weight.

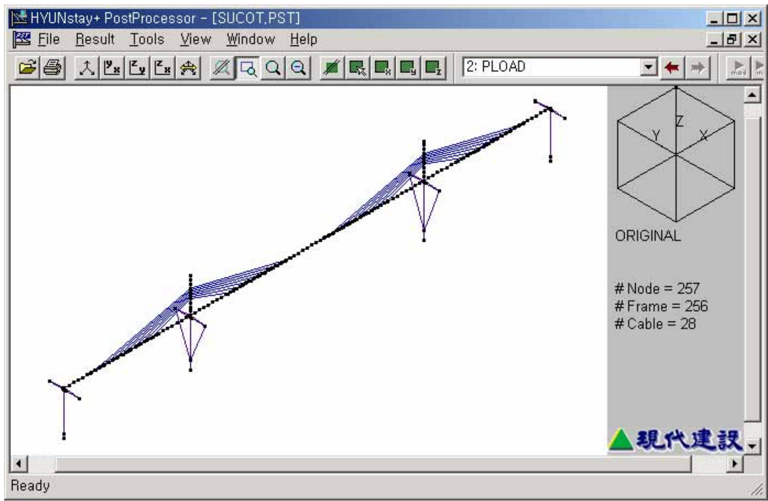

Fig. 4 Modeling of bridge by HYUNSTAY.

FREE FIELD MOTION

Modeling of the ground

Figure 5 shows the bridge crossing ground which is consisted of sand, weathered rock, soft rock and crushing rock along the fault. Crushing rock region along the fault has relatively low shear velocity and its influence on free field motion must be considered. The material properties of ground are provided in table 1.

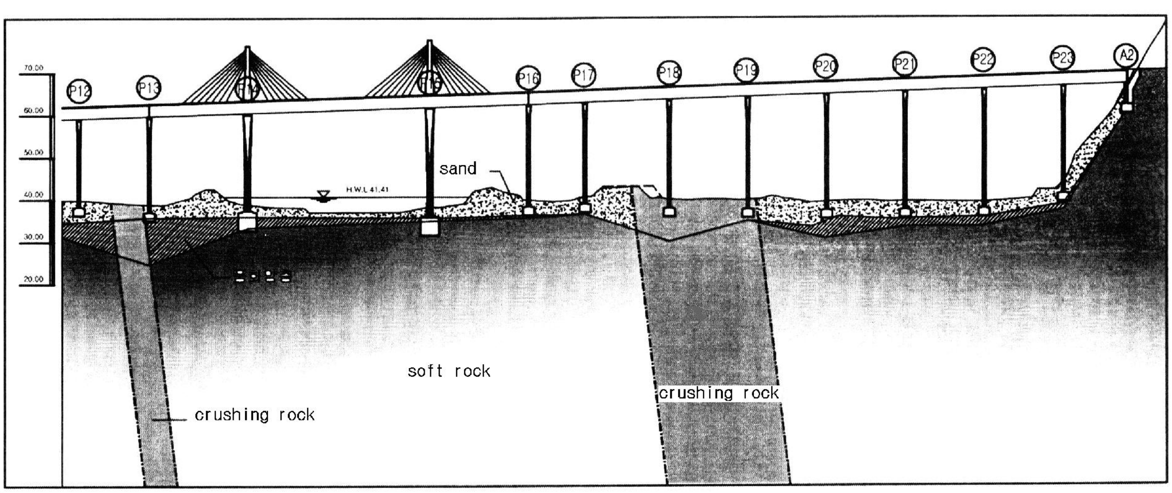

Fig. 5 Overview of bridge and ground.

Table 1 Material properties of ground.

	shear velocity $V_S\ (m/\sec^2)$	density $\rho\ (t/m^3)$	Poisson's ratio ν	damping ratio ξ
Sand	210.0	1.9	0.425	0.05
Weatherd rock	430.0	2.1	0.371	0.05
Soft rock	750.0	2.3	0.347	0.05
Crushing rock	270.0	2.0	0.423	0.05

Laterally heterogeneous ground is assumed to consist of layered strata over rigid bedrock. The ground is modeled using 2-D hyperelements and finite elements as shown in Figure 6. Region F1~F7 where the piers are standing are modeled using finite elements and strip hyperelements are used to model R1~R7 region. Transmitting boundaries by hyperelements are attached to T1 and T2 region.

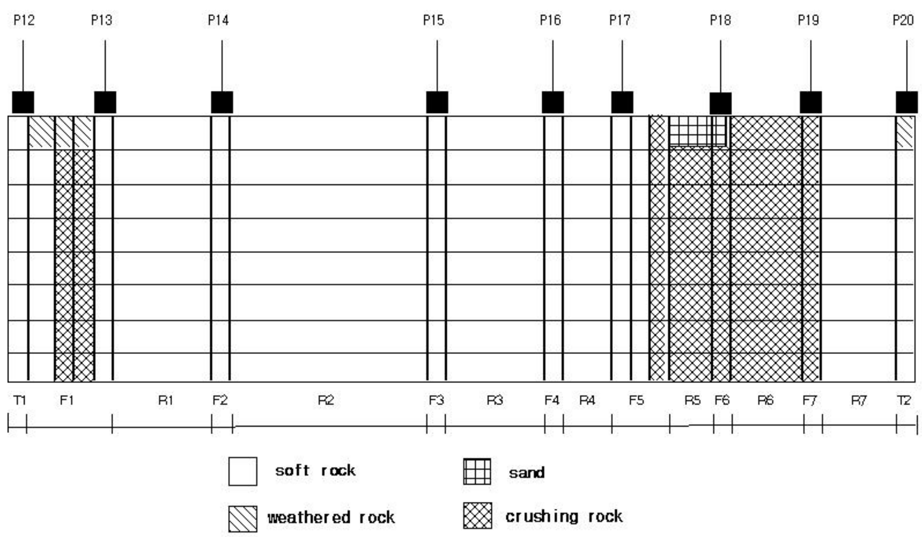

Fig. 6 2-D hybrid modeling of the ground.

Free field motion analysis

The ground motion may be significantly influenced due to the site effects. The free field motion is calculated using the 2-D ground model as Figure 6.

Control motion

Design response spectrum compatible artificial motions are generated and used as control motion. Generated five artificial motions are averaged and its acceleration response spectrum is compared with design response spectrum in Figure 7.

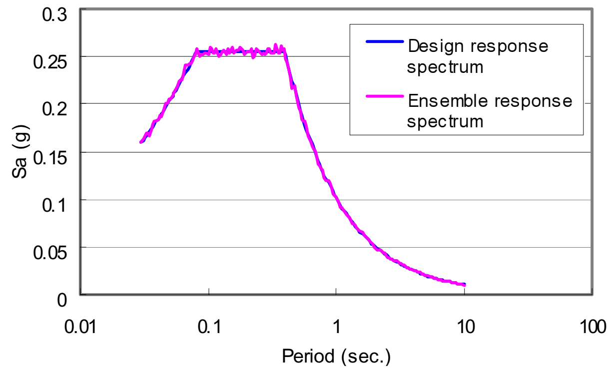

Fig. 7 Acceleration response spectrum of averaged artificial motion.

Free field analysis results

The response spectrums of free field motions at the location of pier 13, 14, 15, 16 in longitudinal and transverse direction are calculated and compared with that of control motion in Figure 8 and Figure 9 respectively. The amplification occurs in high frequency range over 1.0 Hz and is pronounced at the location of pier 13. The ground acceleration amplifies at the location of pier 13 and pier 16 near the crushing rock region and maximum ground acceleration is 0.202g. It is observed that surface ground motion is strongly influenced by the site effect.

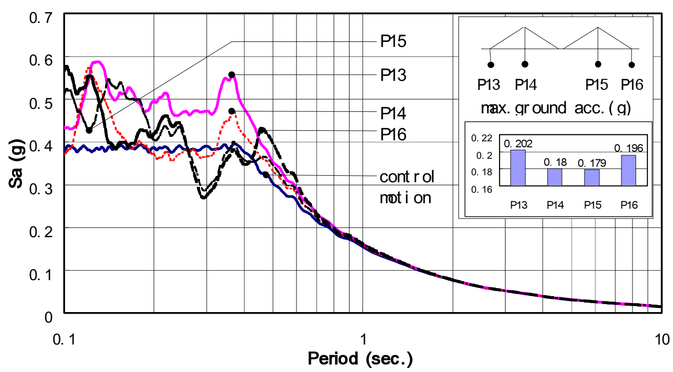

Fig. 8 Comparison of response spectrum in longitudinal direction.

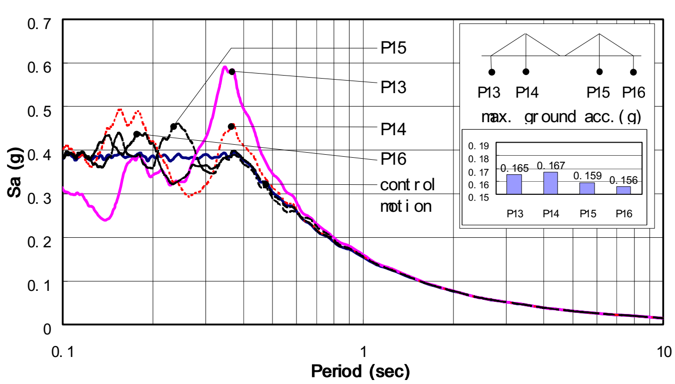

Fig. 9 Comparison of response spectrum in transverse direction.

RESPONSE OF BRIDGE MODEL

The soil-structure interaction effects are taken into account using soil spring. The natural frequencies of first four modes and 10th mode are listed in Table 2 along with the mode classification and it shows the majority of modes are in low frequency range.

Table 2 Modes of SSI bridge model.

mode	period (sec.)	natural freq. (Hz)	classification
1	2.328	0.430	longitudinal
2	2.322	0.431	transverse
3	2.186	0.458	torsion
4	1.959	0.511	bending
10	0.453	2.206	pier only

Responses of bridge model are calculated subjected to the four different kinds of input motion. In the first three cases the base of all the piers are excited with generated artificial motion 1, 2 and 3 respectively. Surface ground motions calculated by free field analysis are used as input motion at the base of each pier in 4th case. Bending moment of piers by longitudinal and transverse input motions are calculated and compared in Figure 10 and 11 respectively. Results show similar or decreasing member force by the surface ground motions considering site effects. Amplification of ground motion occurs in the frequency range over 1.0 Hz as in Figure 8 and 9 but major natural frequencies of bridge are around 0.4 Hz and amplification of member force does not occur.

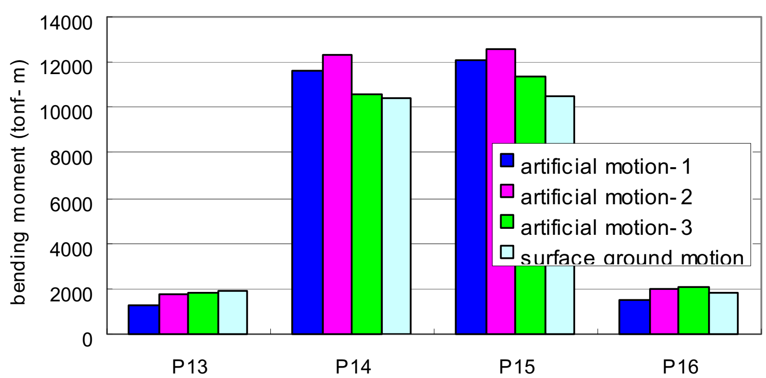

Fig. 10 Member force of pier by longitudinal input motion.

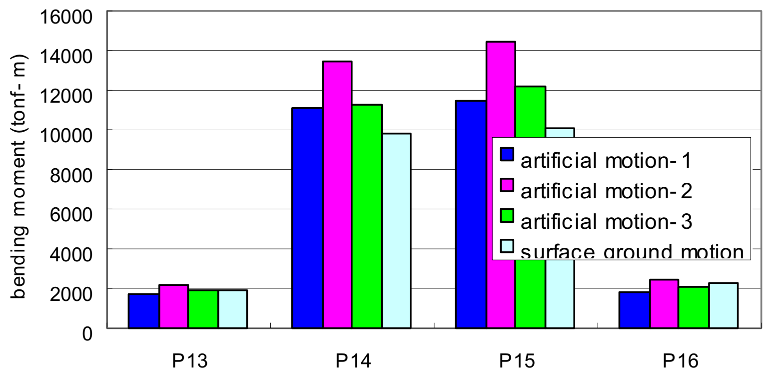

Fig. 11 Member force of pier by transverse input motion.

Figure 12 shows the effect of base isolation system LRB(lead rubber bearing) installed in this bridge. Spectral acceleration decreases from 0.55g at natural frequency of non LRB system to 0.07g at that of LRB installed system.

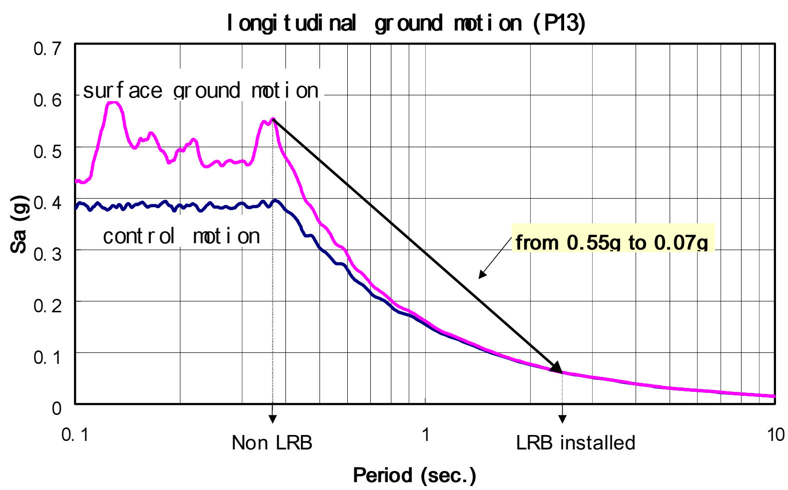

Fig. 12 The effect of base isolation system.

CONCLUSIONS

The ground of irregular geometry and heterogeneous soil profile can be modeled by 3-dimensional hyperelement formulated in Cartesian coordinate system.

The free field analysis results show that the ground motion is significantly influenced due to the site effects. The amplification of ground motion occurs and is pronounced near the location of crushing rock region having low strength.

The major modes of a three-span extradosed bridge exist in low frequency range and the amplification of input motions are restricted within high frequency range. It indicates that the low frequency response of extradosed bridge is not affected by site effects and amplification of member force does not occur.

The influence of amplification of ground motion on the seismic response of bridge can be reduced controlling dominant frequency of bridge by base isolation system like LRB.

REFERENCES

1. Keshishian P., Der Kiureghian A. “Effect of Soil-Structure Interaction on Response to Spatially Varying Ground Motion.” Structural Engineers World Congress, 1998.
2. Kornkasem W., Nam S. I., Foutch A. A., Ghaboussi J., and Aschheim M. A. “Seismic Analysis of a Truss-arch Bridge Crossing the Mississippi River.” 12th World Conference on Earthquake Engineering, 2000.
3. Zembaty Z., and Rutenberg A. “On the Sensitivity of Bridge Seismic Response with Local Soil Amplification.” Earthquake Engineering and Structural Dynamics, 27, 1998: 1095-1099.
4. Kim J. K., Koh H. M., Kwon K. J., and Yi J. S. “A Three-dimensional Transmitting boundary formulated in Cartesian Co-ordinate System for the Dynamics of Non-axisymmetric Foundations.” Earthquake Engineering and Structural Dynamics, 29, 2000: 1527-1546.
5. Waas G. “Linear two-dimensional analysis of soil dynamics problems in semi-infinite layered media.” Ph.D. Dissertation, University of California Berkeley, California, 1972.
6. Yi J. S. “Three-Dimensional Strip Hyperelement for Soil-Structure Interaction Analysis in a Heterogeneous Ground.” Ph.D. Dissertation, Seoul National University, 2001.
7. Hyundai Institute of Construction Technology. “Development of Pre and Post Processor Program for Cable Stayed Bridges.” 98CSTR05, 1999.
8. Nazmy A. S., Abdel-Ghaffar A. M. “Three-Dimensional Nonlinear Static Analysis of Cable-Stayed Bridges.” Computer & Structures, Vol.34, No.2, 1990: 257-271.